Evaluation of Multi-Section Resistive Tapered Stripline (RTS) Lead Wires to Reduce SAR Near Implanted DBS Electrodes During MRI

Peter Serano[1,2], Leonardo M. Angelone[3], and Giorgio Bonmassar[1]

[1]*Athinoula A. Martinos Center for Biomedical Imaging, Charlestown, MA, United States,* [2]*Electrical and Computer Engineering, University of Maryland, College Park, MD, United States,* [3]*U.S. Food and Drug Administration CDRH/OSEL/DP, Silver Spring, MD, United States*

Purpose Despite its remarkable success, one of the significant limitations of Deep Brain Stimulation (DBS) is its limited compatibility with MRI. When performing MRI in patients with DBS implants, one of the major issues is the heating of tissue surrounding the implant due to radiofrequency (RF) pickup of the implant acting as an antenna. We present an extensive evaluation of the design parameters of a novel DBS lead for MRI based on Resistive Tapered Stripline[1] (RTS) technology. The RTS design is characterized by an abrupt variation of conductivity along its length, which creates an impedance mismatch to scatter the energy of the RF wave in the lead. This innovative high scattering technology may allow for decreased lead antenna effect and tissue specific absorption rate (SAR) while maintaining low lead resistance for continuous current injection.

Methods SAR was calculated with numerical simulations based on Finite Elements (ANSYS HFSS v15.0) using an electromagnetic and circuit co-simulation method[2,3]. The model, shown in **Fig. 1 (left)**, included a clinical 3T RF transmit coil loaded with the ASTM phantom[4] and tuned to 128MHz[5]. The input voltage to the coil was adjusted to set a whole-body averaged SAR within the phantom of 2.0 W/kg (Normal Operating Mode for MRI systems[6]). The DBS lead was placed in the area of maximum magnitude of the incident electric field (**Fig. 1, right**.) and the position was kept the same for all the designs analyzed. The RTS lead model consists of a rectangular shaped insulated conductive ink trace with a length of 40cm and an exposed platinum electrode with a length of 1.5mm - each with a width of 0.4mm, and thickness of 10µm. The lead model is portioned into six equal length sections and each was assigned a variable conductivity (**Fig. 2, top**). Designs were defined as a set of six conductivity values. Design values were chosen as to include all possible RTS lead designs where conductivity increases or decreases by a factor of 50x between adjacent sections, thus yielding a pair of conductivity values σ_1 and $\sigma_2 = 50\sigma_1$ to comprise the lead. Specific values of conductivity are then selected to yield a desired total low frequency lead resistance. In each design, the section adjacent to the electrode was defined as the less conductive value as to provide the first impedance mismatch point between the lead and the high conductivity platinum electrode. "RTS-N" lead designs were defined as having N number of changes in conductivity along the length of the lead (**Fig. 2, bottom**). All possible configurations of RTS-N designs for N = 2-6 were derived at R = 400 Ω and simulated. The best configurations which yielded the lowest SAR were then swept across a range of lead resistances from 50Ω to 400Ω. For each lead design simulation, the 10g-averaged SAR was computed at a point 0.1mm from the anterior face of the exposed distal electrode lead contact. L-Curves of SAR vs. lead resistance were generated to evaluate performance (**Fig. 3**).

Results Simulations showed that the use of a two or three section RTS lead each resulted in an average 38% decrease of 10g-averaged SAR across all resistances when compared to a resistively homogeneous stripline (RHS) (**Fig. 3**). By increasing the number of RTS sections to four, an additional 5% reduction (40% total SAR reduction) in SAR averaged across the range of resistances was achieved. SAR reduction performance was reduced across all resistances when increasing beyond four sections.

Conclusion The multi-section RTS design can allow for a significant reduction in 10g-averaged SAR at the distal electrode. RTS may be able to directly replace traditional implanted leads and the high RF-attenuation can reduce SAR and improve subject safety. An additional advantage over traditional lead design is that RTS does not require any RF components (e.g., RF chokes) which are difficult to incorporate in the restricted space of a microscopic wire and are susceptible to failure over time.

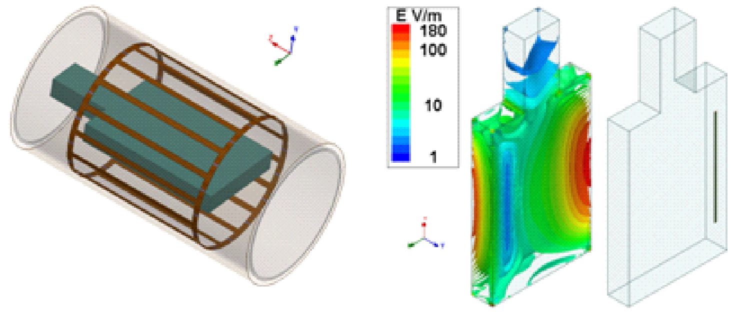

Figure 1: (left) The CAD Model used in the simulations including a 16-rung high-pass birdcage body coil with shield, coil former, and ASTM phantom. (right) Complex magnitude of the electric field at the Larmor frequency in an ASTM phantom. The lead placement in the phantom is shown in the same coordinate system to the right.

<table>
<tr><th></th><th>σ1 , L1</th><th>σ2 , L2</th><th>σ3 , L3</th><th>σ4 , L4</th><th>σ5 , L5</th><th>σ6 , L6</th></tr>
<tr><td>1</td><td colspan="6">σ1</td></tr>
<tr><td>2</td><td>σ2</td><td colspan="5">50 σ2</td></tr>
<tr><td>3</td><td>σ3</td><td colspan="3">50 σ3</td><td colspan="2">σ3</td></tr>
<tr><td>4</td><td>σ4</td><td colspan="3">50 σ4</td><td>σ4</td><td>50 σ4</td></tr>
<tr><td>5</td><td>σ5</td><td colspan="2">50 σ5</td><td>σ5</td><td>50 σ5</td><td>σ5</td></tr>
<tr><td>6</td><td>σ6</td><td>50 σ6</td><td>σ6</td><td>50 σ6</td><td>σ6</td><td>50 σ6</td></tr>
</table>

Figure 2: (top) Generic RTS lead design consisting of six sections that can be assigned a variable length and conductivity. (bottom) Found best performing RTS lead configurations for each respective N-section design.

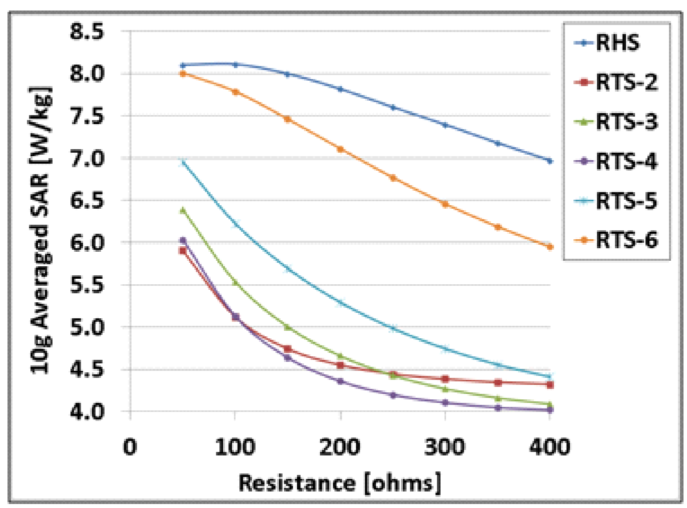

Figure 3: 10g-averaged SAR at the distal electrode vs. total lead resistance obtained for the Resistively Homogeneous Stripline (RHS) and two to six section RTS designs.

References [1] G. Bonmassar. IEEE Transactions of MTT vol. 52, pp. 1992-1998 (2004). [2] M. Kozlov, and R. Turner, JMRI vol. 200, pp. 147-152 (2009). [3] R. Lemdiasov, A. Obi, and R. Ludwig, CMR vol. 38A, no. 4, pp. 133-147 (2011). [4] ASTM, Standard F2182-11a, (2011). [5] G. Bonmassar, et. al., Proc. IEEE EMBS NEC (2013). [6] IEC 601-2-33: Part 2-33, 2nd revision 2010.